The Astrophysical Journal, 572:996–1001, 2002 June 20
© 2002. The American Astronomical Society. All rights reserved. Printed in U.S.A.

IS RX J1856.5−3754 A QUARK STAR?

Jeremy J. Drake,[1] Herman L. Marshall,[2] Stefan Dreizler,[3] Peter E. Freeman,[1] Antonella Fruscione,[1]
Michael Juda,[1] Vinay Kashyap,[1] Fabrizio Nicastro,[1] Deron O. Pease,[1]
Bradford J. Wargelin,[1] and Klaus Werner[3]
Received 2001 December 15; accepted 2002 February 21

ABSTRACT

Deep *Chandra* Low Energy Transmission Grating and High Resolution Camera spectroscopic observations of the isolated neutron star candidate RX J1856.5−3754 have been analyzed to search for metallic and resonance cyclotron spectral features and for pulsation behavior. As found from earlier observations, the X-ray spectrum is well represented by an ∼60 eV (7×10^5 K) blackbody. No unequivocal evidence of spectral line or edge features has been found, arguing against metal-dominated models. The data contain no evidence for pulsation, and we place a 99% confidence upper limit of 2.7% on the unaccelerated pulse fraction over a wide frequency range from 10^{-4} to 100 Hz. We argue that the derived interstellar medium neutral hydrogen column density of 8×10^{19} cm$^{-2} \leq N_{\rm H} \leq 1.1 \times 10^{20}$ cm^{-2} favors the larger distance from two recent *Hubble Space Telescope* parallax analyses, placing RX J1856.5−3754 at ∼140 pc instead of ∼60 pc and in the outskirts of the R CrA dark molecular cloud. That such a comparatively rare region of high interstellar matter (ISM) density is precisely where an isolated neutron star reheated by accretion of ISM would be expected is either entirely coincidental or current theoretical arguments excluding this scenario for RX J1856.5−3754 are premature. Taken at face value, the combined observational evidence—a lack of spectral and temporal features and an implied radius of $R_\infty = 3.8$–8.2 km that is too small for current neutron star models—points to a more compact object, such as allowed for quark matter equations of state.

Subject headings: stars: individual (RX J1856.5−3754) — stars: neutron — X-rays: stars

1. INTRODUCTION

The structure and evolution of neutron stars depends on the properties of matter at nuclear and supranuclear densities. Such conditions are not achievable in terrestrial laboratories and the theoretical description of such superdense matter remains uncertain. It has therefore been hoped that neutron stars, in particular those that are isolated and not complicated by strong accretion or magnetospheric signatures, might provide some empirical insights: observations of their masses, radii, and cooling characteristics could, in principle, provide useful constraints for the equation of state (EOS) of dense matter (e.g., Lattimer & Prakash 2001 and references therein).

In a relatively brief period of 10^6–10^7 yr, a hot, isolated neutron star (INS) born in a supernova explosion can cool, cease pulsar activity, and become essentially inactive (see, e.g., the review of Treves et al. 2000). Of the estimated 10^8–10^9 isolated neutron stars thought to inhabit the Galaxy, only a tiny fraction are therefore expected to be sufficiently young to remain hot and visible in X-rays. One possible mechanism capable of sustaining thermal X-ray emission in an older INS is accretion of material from the interstellar matter (ISM). To date, only a handful of these older INS candidates have been found.

The soft X-ray source RX J1856.5−3754 discovered by Walter, Wolk, & Neuhäuser (1996) is the brightest and probably the closest (Kaplan, van Kerkwijk, & Anderson 2002) of the INS candidates. It was identified with a very faint ($V \simeq 25.6$) optical counterpart by Walter & Matthews (1997), was found to have an optical flux about a factor of 2–3 higher than that predicted by the Rayleigh-Jeans tail of the ∼55 eV blackbody spectrum that represents the low resolution *ROSAT* Position Sensitive Proportional Counter (PSPC) spectrum (e.g., Walter et al. 1996; Campana, Mereghetti, & Sidoli 1997; Pons et al. 2002), and lies in the line of sight toward the dark molecular cloud R CrA. However, the exact nature of RX J1856.5−3754 remains unknown—whether it is a fairly young, cooling INS, perhaps undetected as a pulsar because of unfortunate beam alignment, or an older object reheated by ISM accretion.

Very Large Telescope (VLT) observations have recently revealed an Hα nebula around RX J1856.5−3754 and a blackbody spectrum through the UV-optical range (van Kerkwijk & Kulkarni 2001a, 2001b). *Hubble Space Telescope* (*HST*) astrometry was used by Walter (2001) and Kaplan et al. (2002) to estimate a parallax and proper motion, but with conflicting results (16.5 ± 2.3 mas vs. 7 ± 2 mas). Walter (2001) argued that the proper motion points to the Sco-Cen OB association and an age of $\sim 10^6$ yr. However, Pons et al. (2002) failed to detect the expected pulsation signature in *ROSAT* and *ASCA* data. Modeling X-ray, EUV, UV, and optical spectra using the Walter (2001) parallax and assuming a metal-dominated atmosphere resulted in stellar radii too small for the current EOS and smaller than the Schwarzschild radius for a canonical 1.4 $M_\odot$ star, leading them to conclude that the surface temperature distribution could be inhomogeneous. In contrast, the same atmospheric analysis using the larger distance of Kaplan et al. (2002) would yield a radius consistent with current theory. If the atmosphere is indeed metal-dominated, then line and edge features should be visible in high-resolution X-ray spectra.

[1] Smithsonian Astrophysical Observatory, MS 3, 60 Garden Street, Cambridge, MA 02138.
[2] Massachusetts Institute of Technology Center for Space Research, 77 Massachusetts Avenue, Cambridge, MA 02139.
[3] Institut für Astronomie und Astrophysik, Universität Tübingen, Sand 1, 72076 Tübingen, Germany.

TABLE 1
SUMMARY OF *Chandra* LETG+HRC-S OBSERVATIONS

ObsID	UT Start	UT End	Exposure (s)	Net Events[a] Zeroth	Net Events[a] Zeroth + First	Zeroth Rate[b] (Hz)
113.....	2000 Mar 10 07:55:12	2000 Mar 10 23:37:24	55121	12202	...	0.2195 ± 0.0020
3382.....	2001 Oct 8 08:18:49	2001 Oct 9 03:01:50	101172	20949	86516	0.2166 ± 0.0016
3380.....	2001 Oct 10 05:06:28	2001 Oct 12 04:00:48	166325	35097	135230	0.2154 ± 0.0013
3381.....	2001 Oct 12 19:19:26	2001 Oct 14 09:14:28	169956	36011	141349	0.2157 ± 0.0013
3399.....	2001 Oct 15 11:47:06	2001 Oct 15 14:42:59	9282	1962	7136	0.2126 ± 0.0051

[a] The net event numbers include background events; while including the first-order events increases the net source events, the number of background events also increases.
[b] Rates were derived from zeroth-order data when valid event rates did not exceed 184 counts s^{-1}; this selection criterion yielded 417,786 s of the 501,856 s total exposure time.

RX J1856.5−3754 was observed in 2000 March for 55 ks by the *Chandra X-Ray Observatory* Low Energy Transmission Grating (LETG) and the High Resolution Camera spectroscopic (HRC-S) microchannel plate detector array to look for spectral features and pulsar activity. Within relatively large statistical uncertainties, Burwitz et al. (2001) failed to detect either significant departures from a blackbody spectrum or pulsations in these data. The prospect of important scientific gains from a longer observation prompted, at the request of different researchers, the undertaking of a very recent set of *Chandra* observations of RX J1856.5−3754 under the director's discretionary time using LETG+HRC-S. A period search using these data by Ransom, Gaensler, & Slane (2002) has already placed an upper limit on a pulse fraction of 4.5%. This paper presents spectroscopic and independent timing analyses of these data.

2. OBSERVATIONS AND DATA REDUCTION

The observations analyzed in this paper are summarized in Table 1. Pipeline-processed (CXC software version 6.3.1) photon event lists were reduced and analysed using the CIAO software package version 2.2 and independently using custom IDL[4] software. Processing included extra pulse-height filtering to reduce background (B. J. Wargelin et al. 2002, in preparation) and barycentric correction of event times. Dispersed photon events were extracted using the now standard "bow tie" window, and a small circular region (31 pixel radius[5]) was used to extract the zeroth-order events. We note that an extraneous bright feature (likely a ghost image of a bright off-axis source) appeared on the +1 order outer HRC-S plate, which introduces spurious features into the extracted spectrum and background near 110 Å. We applied corrections to extracted event times to ameliorate an HRC electronics problem that assigns time tags for each event to the event that immediately follows. If every event were telemetered to the ground, correct times could be easily reassigned, but because of the high HRC background rate and a telemetry limit of 184 events s^{-1}, only *valid* events, which make up approximately 45% of the *total* events in these observations, are recorded in data received on the ground. We have reassigned the time of every valid event to the preceding valid event during ground processing; the event times will then be correct about $N_{\rm valid}/N_{\rm total}$ of the time. One can place an upper limit of δt on the time errors associated with this process, however, simply by excluding events with a time shift of more than δt; the average timing error of such events will, of course, be less than δt. However, if δt is too small, too many events get excluded to perform sensitive timing studies. We have adopted a δt of 2 ms, retaining 20% of the original counts in the corrected data set.

3. COUNT RATES AND TIMING ANALYSIS

Count rates were derived for each observation segment from event lists filtered to exclude times of high background and telemetry saturation, when the telemetered valid event rate exceeded 184 count s^{-1}, and to exclude high pulse-height events that arise entirely from background. These rates corresponding to zeroth order only are listed in Table 1.

The count rates for the different observation segments are statistically consistent, though the 2000 March observation (observation identification [ObsID] 113) rate of 0.2195 ± 0.0020 count s^{-1} lies 1.9% and 1.9 σ above the rate for the combined 2001 October series rate of 0.2155 ± 0.0008. Such deviations will be obtained by chance about 3% of the time when the count rates do not vary; it is thus more likely attributable to quantum efficiency (QE) variations in the detector on small scales. Indeed, Pons et al. (2002) note two *ROSAT* HRI observations obtained 3 years apart that are consistent to 1%. The fluxes corresponding to HRI and PSPC count rates are higher than that obtained from our *Chandra* data by 20% and 30%, respectively. As remarked by Burwitz et al. (2001), these differences are likely attributable to absolute calibration uncertainties. We have also examined the *ASCA* Solid State Imaging Spectrometer (SIS) observation described by Pons et al. (2002) and find fluxes 30%–40% lower than those obtained by *Chandra* for the 20–30 Å range, but in agreement with *Chandra* shortward of 20 Å. The *Extreme Ultraviolet Explorer* Deep Survey count rate of Pons et al. (2002) is also consistent with the *Chandra* observation within allowed uncertainties.

Our search for pulsations used three different techniques, none of which found any evidence for significant variability. In contrast to Ransom et al. (2002), we did not include a deceleration term; this will be discussed below.

[4] Interactive Data Language, Research Systems Inc.
[5] Our 31 pixel radius extraction region for the zeroth-order source corresponds to an encircled energy fraction of about $92\% \pm 3\%$, which combines with an average deadtime of 0.59% to yield a correction factor for a 2π sr aperture of 1.09.

We applied the Bayesian method of Gregory & Loredo (1992) to both the time-corrected and uncorrected zeroth-order event lists. The method tests for variability by comparing the fits of periodic stepwise models to the data with the fit of a constant model. The odds favoring variability (based on eq. [5.28] of Gregory & Loredo 1992, with a maximum number of steps $m_{\max} = 12$ and limiting angular frequencies $\omega_{\rm lo}$ and $\omega_{\rm hi}$ equal to 10^{-4} and 10^{3}, respectively) were found to be 1.45×10^{-4} for the whole data set and 3.75×10^{-3} for the data filtered on $\delta t = 2$ ms, both to be compared with an odds value of 10^2 needed for a confident pulsation or variability detection.

Our second method employed a fast Fourier transform (FFT) analysis applied to the combined zeroth and first-order events, followed by a likelihood ratio test (LRT) to determine limits on the pulse fraction. The FFT power distribution was consistent with shot noise. For the LRT of a given period, P, the data were binned into N phase bins, giving n_i counts in each. The source model was $y = A + f\cos(\phi_i + \phi_0)$, where ϕ_i is the phase of bin i and ϕ_0 is the phase of the pulse and f/A is the pulse fraction. The likelihood equations were then solved for A and the process applied to greater than 500 frequencies where the FFT power exceeded a critical level in the frequency range of 0.001–50 Hz. By also including the dispersed events, we improved the signal-to-noise ratio of the result by a factor of 1.47 compared with using the zeroth order alone, and we could obtain a pulse fraction limit lower than the value of 4.5% obtained by Ransom et al. (2002) in their unaccelerated search. A pulse fraction upper limit (99% confidence) of 2.7% was derived applying our likelihood ratio method using all data, including the dispersed events with $1\ \text{Å} < \lambda < 70$ Å. Taking only the events limited by $\delta t < 2$ ms, the pulse fraction limit is 10%.

Third, we computed the Lomb-Scargle periodogram for both the time-corrected and uncorrected photon arrival time differences in the frequency range of 0.01–1 Hz for the events in ObsID 3380, 3381, 3382, and 3399. Again, no significant peaks were present.

The assumption of a negligible deceleration term in our period search restricts the range of periods and dipole magnetic field strengths for which our search is valid. The coherence limit for phase slippage by 10% over the duration of the 2001 October observations implies that our result is valid for a magnetic field upper limit of $B < 2.3 \times 10^{13} P^{3/2}$ G for period P s (e.g., Shapiro & Teukolsky 1983). As noted by Ransom et al. (2002), this range would exclude very young and energetic neutron stars, such as the Crab and Vela pulsars, though most of these younger objects are also conspicuously strong radio pulsars. All anomalous X-ray pulsars would lie within our sensitivity limit range. RX J1856.5−3754 is also most unlikely to be an extremely young object based on its modest temperature and luminosity, which are consistent with an object of age $\sim 10^5$ yr on canonical cooling curves (e.g., Tsuruta 1997).

4. SPECTRAL ANALYSIS AND MODEL PARAMETER ESTIMATION

Spectral analysis in the form of model parameter estimation was undertaken using the CIAO Sherpa fitting engine and independently using specially written IDL software. Cursory inspection of the spectrum leads immediately to the conclusion that there are no obvious features indicative of absorption lines or edges. We found that blackbody models represent the high-resolution spectra well, in agreement with earlier studies. We modeled +1 and −1 orders both separately and simultaneously and added together; results from these different approaches were statistically indistinguishable. Representative results of model fits and residuals are illustrated in Figure 1. Two sets of best-fit parameters were obtained from independent analyses that invoked (1) the existing first- and higher order CXC calibration[6] and (2) the same first-order effective area with higher orders modified slightly to improve model fits to sources with power-law spectra (H. L. Marshall et al. 2002, in preparation). Both sets are consistent with the results of Burwitz et al. (2001) based on the 2000 March observation alone. Parameters and 1 σ statistical uncertainties for best-fit models were: (1) $T = 61.2 \pm 0.3$ eV, $N_{\rm H} = (1.10 \pm 0.02) \times 10^{20}$ cm^{-2}, X-ray luminosity $(2.96 \pm 0.03) \times 10^{31} D_{100}^2$ ergs s^{-1}, where D_{100} is the distance in units of 100 pc, (2) $T = 61.1 \pm 0.3$ eV, $N_{\rm H} = (0.81 \pm 0.02) \times 10^{20}$ cm^{-2}, X-ray luminosity $(3.16 \pm 0.03) \times 10^{31} D_{100}^2$ ergs s^{-1}. Parameters producing minima in the χ^2 test statistic were not sensitive to the exact binning adopted, though of course the reduced χ^2 values were the following: values ranged from 0.94 for data binned to a signal-to-noise ratio of S/N = 10 to 1.7 for S/N = 30. The latter value is dominated by residual effective area calibration uncertainties. To investigate the effects of these uncertainties, which are estimated to be about 15% absolutely, a first-order polynomial term was included in the source model to mimic an effective area lower by 15% at 20 Å and higher by 15% at 100 Å and vice versa. Such a slope skews the blackbody curve and leads systematically to

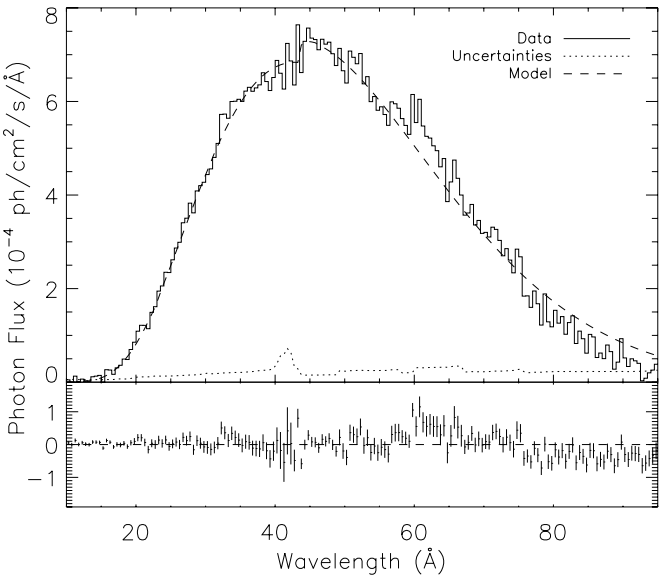

FIG. 1.—Combined positive and negative order spectra of RX J1856.5−3754 binned at 0.5 Å intervals, shown with the best-fit blackbody model with parameters corresponding to method 2 in § 4 and residuals (observations−model). The deviations from this model are consistent with Poisson statistics after allowing for calibration uncertainties at the C K edge and over broader wavelength intervals. The apparent edge at 60 Å results primarily from one of the HRC-S plate gap boundaries and small residual QE differences between positive- and relative negative-order outer plates.

[6] Version dated 2000 October 31, available on-line at http://asc.harvard.edu/cal/Links/Letg/User.

higher or lower temperature solutions by about 1 eV—clearly the true temperature uncertainty is driven by this uncertainty in the effective area. Allowing for this uncertainty, we adopt a final temperature of 61.2 ± 1.0—in agreement with, but much more tightly constrained than, the *ROSAT* temperatures derived by Burwitz et al. (2001; 63 ± 3 eV) and Pons et al. (2002; 55.3 ± 5.5). We note that a temperature of 61 eV results in an optical flux about a factor of 2 lower than that for a 55 eV blackbody, so that the discrepancy between the observed optical flux and that predicted by the hot blackbody noted by Walter & Matthews (1997) and Pons et al. (2002) is larger by a similar factor. However, this optical flux decrement represents only a small fraction of the total luminosity of RX J1856.5−3754.

Blackbody models were found by both Pons et al. (2002) and Burwitz et al. (2001) to represent observed spectra better than sophisticated model atmospheres, though a uniform-temperature blackbody model was formally excluded in X-ray–EUV–UV–optical modeling in the former work. However, additional cooler components were found to contribute at most only a few percent to the observed *ROSAT* PSPC X-ray flux. We have ruled out the significant presence of additional thermal and nonthermal emission components by trial of models combining two blackbodies and models using a blackbody component with arbitrary power laws: in both cases the additional components were completely unconstrained and resulted in no improvement in the goodness of the fit. The 3 σ upper limit to power-law flux is $5.2 \times 10^{28} D_{100}^2$ ergs s^{-1} keV^{-1} at 1 keV. Our blackbody models from methods 1 and 2 correspond formally to a radius over distance ratio (angular size) of $R_\infty / D_{100} = 4.12 \pm 0.68$ km per 100 pc, where $R_\infty = R/(1 - 2GM/Rc^2)^{1/2}$ is the "radiation radius" corresponding to the true radius R for a star of mass M, and the quoted uncertainty represents the combined temperature determination uncertainty (± 1 eV) and the (dominant) absolute effective area uncertainty of the LETG+HRC-S combination ($\pm 15\%$).

In all model comparisons for binning at S/N > 10 the residual differences between the observed counts and the best-fit model show systematic departures from normal statistical deviations (Fig. 1). Broad deviations are characterized by a general overprediction of observed counts for $\lambda < 30$ Å and in the region of 75–100 Å, which is dominated by higher order flux, underprediction by an average of $\sim$10% for the range of 25–38 Å and deviations around the instrumental C K-edge region of 40–44 Å. The latter results from a residual calibration error in the HRC-S UV/ion shield. Other deviations could arise either as a result of impropriety of a blackbody model for RX J1856.5−3754, or through calibration errors, which are currently estimated to be $\leq$15% over broad spectral ranges and less over narrower ranges (J. J. Drake et al. 2002, in preparation). An apparent edge at 60 Å and flux excess in the range 60–70 Å arises because of one of the HRC-S plate gap boundaries coincides with small residual QE differences between positive and relative negative order outer plates.

In the case of narrow line or edge features, in different combinations of spectral order, data reduction method, and binning size, we identify possible structure in residuals at 26.5, 27.6, 34.4, 32.4, and 35.9 Å (emission-like features), and at 28.2, 39.1, and 86.5 Å (absorption-like features), that might be tempting to attribute to the source. However, we cannot exclude the possibility that any are chance fluctuations at the 1% level. The issue is complicated by possible calibration uncertainties on smaller scales, believed to be at a level of about 5% or less, that should be largely smoothed out by dither. We have also used a 60 ks observation (ObsID 331) of PKS 2155−304, currently thought to be a featureless continuum in the spectral range we are concerned with here (H. L. Marshall et al. 2002, in preparation), as a flat-field source to aid in feature identification. This spectrum comprises about 8 times the number of first-order counts of the combined RX J1856.5−3754 data. Moreover, we have imposed a constraint that features must appear in both positive and negative orders in the RX J1856.5−3754 spectrum. We examined deviations from the model on scales up to 3 Å and find only the expected normal distribution of residuals after allowing for smooth departures resulting from calibration. The Kolmogorov-Smirnov test applied to deviations on different scales also revealed no evidence of significant features at these scales. In summary, all significant deviations that have been found in the residuals can reasonably be explained by instrumental effects. Equivalent width upper limits were derived by applying counting statistics to a convolution of the spectrum with a triangular kernel (Fig. 2).

5. INTERSTELLAR MEDIUM ABSORPTION

The distance of 62 pc derived by Walter (2001) seems at odds with the neutral H column density, $N_{\rm H}$, of 10^{20} cm^{-2} derived from the *Chandra* spectra: measured $N_{\rm H}$ values for objects at this distance based on different techniques are typically in the range of 10^{18}–10^{19} cm^{-2} (e.g., Fruscione et al. 1994). Walter (2001) indeed remarked on this, citing reddening values E_{B-V} of up to 0.1 derived by Knude & Høg (1998) in support of the distance. However, these reddening values show considerable scatter at low reddening and are based only on a relatively coarse attribution of spectral type to the stars considered.

We have estimated $N_{\rm H}$ and the mean local neutral hydrogen number density, $n_{\rm H}$, in the line of sight toward RX J1856.5−3754 as a function of distance by spatial interpolation in the measurements compiled by Fruscione et al. (1994) and Diplas & Savage (1994) using a technique developed by P. Jelinsky (1994, unpublished). We illustrate this

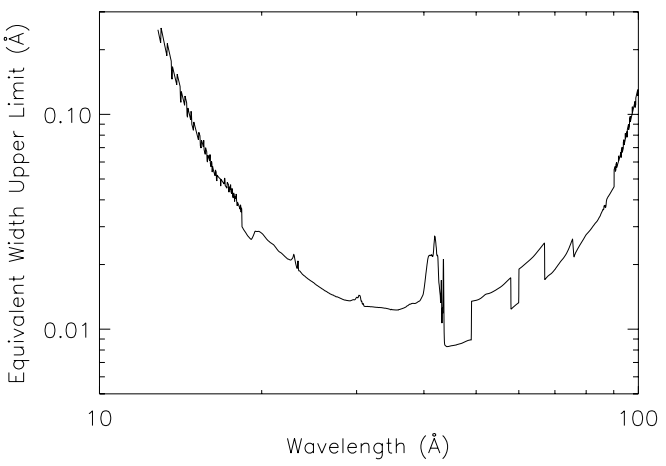

FIG. 2.—The 3 σ equivalent width upper limit to line features as a function of wavelength, based on a convolution of the spectrum with a triangular kernel.

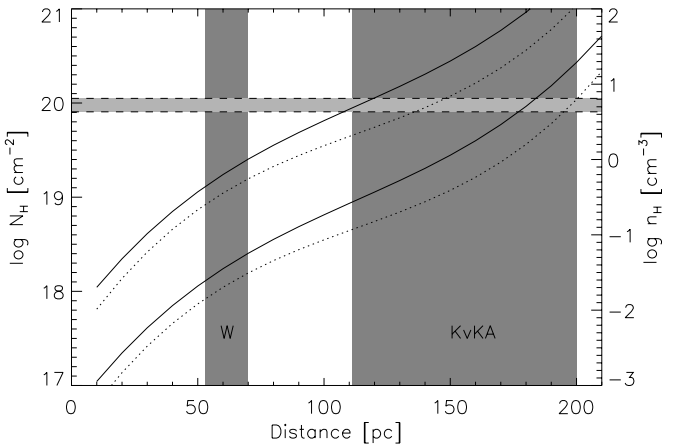

FIG. 3.—The estimated N_H (*solid curves*) and n_H (*dotted curves*) as a function of distance in the line of sight toward RX J1856.5−3754. The pairs of curves represent the likely ranges of these quantities and correspond to deviations of factors of 3 from a smooth locus through the results of the three-dimensional interpolations. Vertical shaded regions indicate the distance ranges found by Walter (2001; W) and Kaplan et al. (2002; KvKA). The horizontal stripe illustrates the allowed range ($\pm 1\ \sigma$) of N_H derived in this study.

in Figure 3, together with the allowed distance ranges from Walter (2001) and Kaplan et al. (2002). The value of N_H estimated in this way at a distance of 60 pc is an order of magnitude lower than the X-ray measurement, but is in good agreement with the distance of 140 pc derived by the latter authors. This distance would place RX J1856.5−3754 on the outskirts of the R CrA cloud using the cloud distance of Knude & Høg (1998) of ∼170 pc and within the cloud using the canonical cloud distance of ∼130 pc. In either case, RX J1856.5−3754 would likely lie in a region of relatively high ISM density (∼1–10 cm^{-3}). While these estimates of N_H are crude and will smooth out any small-scale ISM inhomogeneities, the larger distance is easier to reconcile with the measured column. The cloud distance of Knude & Høg (1998) then represents an upper limit to the distance of RX J1856.5−3754.

6. DISCUSSION

Our results, combined with the recent analysis of Ransom et al. (2002), demonstrate a lack of pulsed features above a level of 2.7% (unaccelerated search; 4.5% from the accelerated search of Ransom et al. 2002) and no unequivocal detection of spectral features. This dearth of indices with which to restrict parameter space precludes an obvious answer to the problem of the nature and origin of RX J1856.5−3754.

The apparent lack of electron or proton resonance cyclotron absorption suggests that magnetic field strengths in the ranges of $(1–7) \times 10^{10}$ and $(0.2–1.3) \times 10^{14}$ G are less likely, as discussed by Paerels et al. (2001) for RX J0720.4−3125 and by Burwitz et al. (2001), but, as emphasized by the latter, they should not be excluded owing to possible difficulties in detecting the absorption features. Indeed, neutron stars with different levels of magnetic field up to 10^{15} G have now been observed with high-resolution X-ray spectrometers and none have so far shown absorption features that are intrinsic to the stellar photosphere (e.g., RX J0720.4−3125, Paerels et al. 2001; PSR 0656+14, Marshall & Schulz 2002; Vela, Pavlov et al. 2001; and 4U 0142+61, Juett et al. 2001).

Our derived angular size based on modeling of the LETGS spectra, $R_\infty / D_{100} = 4.12 \pm 0.68$ km per 100 pc, is consistent with that of Burwitz et al. (2001), though the revised allowed distance range of 111–200 pc (Kaplan et al. 2002), together with the distance upper limit constraint based on the R CrA cloud, $D_{100} \leq 1.70$, now implies a radiation radius in the range of $R_\infty = 3.8–8.2$ km. The high end of this range, corresponding to the largest allowed distance, is still inconsistent with current "normal" NS equations of state ($R_\infty \gtrsim 12$ km; e.g., Lattimer & Prakash 2000), as well as with those with extreme softening, such as kaon condensate models.

Pons et al. (2002) find that heavy element-dominated atmosphere models provide a plausible match to the low-resolution *ROSAT* PSPC spectra and UV and optical fluxes of RX J1856.5−3754, while Kaplan et al. (2002) alleviate conflicts with standard EOS through their revised distance. The heavy element models yield larger radii by virtue of having cooler effective temperatures than blackbody spectra with similar energy distributions. However, Burwitz et al. (2001) argued against such uniform-temperature heavy-element–dominated atmosphere solutions based on a lack of the expected spectral line features. The apparently featureless but much higher quality LETGS spectra presented here strengthen these conclusions.

An alternative favored by Pons et al. (2002), Burwitz et al. (2001), and Ransom et al. (2002) is a nonuniform-temperature model—that we are only seeing a localized hot region on the surface of a cooler star. The latter authors argue that the gravitational smearing effects described by Psaltis, Özel, & DeDeo (2000) account for a lack of observed pulsations. However, the pulse fraction expectations of Psaltis et al. (2000) indicate X-ray pulse fraction levels below our 2.7% limit would be seen only ∼10%–15% of the time.

Pulsation would also be expected for a young (∼10^6 yr), cooling INS with a strong magnetic field. The alternative—that RX J1856.5−3754 is an older object reheated by ISM accretion—has been dismissed by Kaplan et al. (2002) and van Kerkwijk & Kulkarni (2001a), largely based on a Bondi-Hoyle accretion rate for the space velocity of Walter (2001) and Kaplan et al. (2002) that would be much too low to explain the observed luminosity and on a possibly strong, accretion-inhibiting magnetic field (Pons et al. 2002). Nevertheless, RX J1856.5−3754 appears to be in the outskirts of the R CrA cloud and, based on its *HST*-derived velocity vector, has likely passed through more dense regions than the one it now resides in. Finding one of only a handful of INS candidates in such a region by chance is very unlikely, yet it is just such dense ISM regions that are expected to power accretion-heated INSs. Based on the large velocity, however, accretion could only be significant if the Bondi-Hoyle formalism were to be inapplicable for RX J1856.5−3754. While we tentatively ascribe the ∼2% change in observed zeroth-order count rate in the 19 months separating the two observation sets to detector effects, such variability could be accommodated by an accretion model as the star passed through ISM density fluctuations on ∼AU scales.

The lack of spectral features is also consistent with a pure hydrogen atmosphere model that is expected to result from modest accretion, whereby heavier elements undergo rapid gravitational settling. Pons et al. (2002) argue that standard pure H models overpredict the optical flux of

RX J1856.5−3754 by a factor of 30 and that the magnetic accreting models of Zane, Turolla, & Treves (2000), while capable of reproducing the observed X-ray–to–optical flux ratio, would need to be 2 orders of magnitude brighter and an order of magnitude hotter than observed. However, different accretion scenarios and atmospheric models might bear examination in light of the otherwise coincidental location of RX J1856.5−3754.

The slightly unfavorable odds of a nonuniform-temperature model failing to show signs of pulsation leads us to consider a third possibility. Taken at face value, the distance, $N_{\rm H}$, and lack of spectral and temporal features and pulsations favor a more compact object than current NS models permit, but one that is allowed for in strange quark matter solutions (e.g., Lattimer & Prakash 2000; Fraga, Pisarski, & Schaffner-Bielich 2001; Hanauske et al. 2001). There now exists a body of evidence from heavy-ion collision experiments supporting the viability of a quark-gluon plasma (Heinz 2001), and the possible existence of "strange stars" (e.g., Itoh 1970; Bodmer 1971; Collins & Perry 1975; Brecher & Caporaso 1976; Chapline & Nauenberg 1978; Witten 1984; Alcock, Farhi, & Olinto 1986; Haensel, Zudnik, & Schaefer 1986) is perhaps not as speculative as it once was. As noted by Xu (2002) and Pons et al. (2002), such an object would be expected to have an approximately thermal spectrum as we observe (we might then speculate that the optical flux decrement of the 61 eV blackbody spectrum could be ameliorated by a small amount of flux redistribution within a thin crust). Such a suggestion is not unprecedented, and there now exists a small handful of objects whose apparent compactness could be explained if they are composed of quark matter (e.g., Bombaci 1997; Cheng et al. 1998; Li et al. 1995, 1999; Xu, Qiao, & Zhang 1999). Of the existing quark star candidates, RX J1856.5−3754 arguably presents the strongest and most direct case. If this case survives future scrutiny, then the likelihood of such an object being the brightest and closest of the current few INS candidates would add some support to speculation that such a state of matter is a common product of supernovae explosions, or a common phase or endpoint in the evolution of a neutron star (e.g., Alcock et al. 1986; Kapoor & Shukre 2001; Xu, Zhang, & Qiao 2001).

We extend warm thanks to Pete Ratzlaff for invaluable assistance and "wonder scripts" developed at short notice. We also thank members of the CfA High Energy Astrophysics Division for useful comments and corrections, and Fred Walter for pointing out an error in the stated optical flux decrement in an earlier version of the manuscript. The SAO authors were supported by NASA contract NAS 8-39073 to the Chandra X-Ray Center during the course of this research. H. L. M. was supported by NASA contract SAO SV 1-61010.

REFERENCES

Alcock, C., Farhi, E., & Olinto, A. 1986, ApJ, 310, 261
Bodmer, A. R. 1971, Phys. Rev. D, 4, 1601
Bombaci, I. 1997, Phys. Rev. C, 55, 1587
Brecher, K., & Caporaso, G. 1976, Nature, 259, 377
Burwitz, V., Zavlin, V. E., Neuhäuser, R., Predehl, P., Trümper, J., & Brinkman, A. C. 2001, A&A, 379, L35
Campana, S., Mereghetti, S., & Sidoli, L. 1997, A&A, 320, 783
Chapline, G., & Nauenberg, M. 1978, in Ann. NY Acad. Sci., 302, 8th Texas Symp. on Relativistic Astrophysics, 191
Cheng, K. S., Dai, Z. G., Wei, D. M., & Lu, T. 1998, Science, 280, 407
Collins, J. C., & Perry, M. J. 1975, Phys. Rev. Lett., 34, 1353
Diplas, A., & Savage, B. D. 1994, ApJS, 93, 211
Fraga, E. S., Pisarski, R. D. & Schaffner-Bielich, J. 2001, Phys. Rev. D, 63, 1702
Fruscione, A., Hawkins, I., Jelinsky, P., & Wiercigroch, A. 1994, ApJS, 94, 127
Gregory, P. C., & Loredo, T. J. 1992, ApJ, 398, 146
Haensel, P., Zdunik, J. L., & Schaefer, R. 1986, A&A, 160, 121
Hanauske, M., Satarov, L. M., Mishustin, I. N., Stöcker, H. & Greiner, W. 2001, Phys. Rev. D, 64, 3005
Heinz, U. 2001, Nucl. Phys. A, 685, 414
Itoh, N. 1970, Prog. Theor. Phys., 44, 291
Juett, A. M., Marshall, H. L., Chakrabarty, D., Canizares, C. R., & Schulz, N. S., 2002, ApJ., 568, L31
Kaplan, D. L., van Kerkwijk, M. H., & Anderson, J. 2002, ApJ, in press
Kapoor, R. C., & Shukre, C. S. 2001, A&A, 375, 405
Knude, J., & Høg, E. 1998, A&A, 338, 897
Lattimer, J. M., & Prakash, M. 2000, Phys. Rep., 333, 121
———. 2001, ApJ, 550, 426
Li, X.-D., Bombaci, I., Dey, M., Dey, J., & van den Heuvel, E. P. J. 1999, Phys. Rev. Lett., 83, 3776
Li, X.-D., Dai, Z.-G., & Wang, Z.-R. 1995, A&A, 303, L1
Marshall, H. L., & Schulz, N. S. 2002, ApJ, submitted
Paerels, F., et al. 2001, A&A, 365, L298
Pavlov, G. G., Zavlin, V. E., Sanwal, D., Burwitz, V., & Garmire, G. P. 2001, ApJ, 552, L129
Pons, J. A., Walter, F. M., Lattimer, J. M., Prakash, M., Neuhäuser, R., & An, P. 2002, ApJ, 564, 981
Psaltis, D., Özel, F., & DeDeo, S. 2000, ApJ, 544, 390
Ransom, S. M., Gaensler, B. M., & Slane, P. O. 2002, ApJ, 570, L75
Shapiro, S. L., & Teukolsky, S. A. 1983, Black Holes, White Dwarfs, and Neutron Stars (New York: Wiley)
Treves, A., Turolla, R., Zane, S., & Colpi, M. 2000, PASP, 112, 297
Tsuruta, S. 1998, Phys. Rep., 292, 1
van Kerkwijk, M. H., & Kulkarni, S. R. 2001a, A&A, 380, 221
———. 2001b, A&A, 378, 986
Walter, F. M. 2001, ApJ, 549, 433
Walter, F. M., & Matthews, L. D. 1997, Nature, 389, 358
Walter, F. M., Wolk, S. J., & Neuhaüser, R. 1996, Nature, 379, 233
Witten, E. 1984, Phys. Rev. D, 30, 272
Xu, R. X. 2002, ApJ, 570, L65
Xu, R. X., Qiao, G. J., & Zhang, B. 1999, ApJ, 522, L109
Xu, R. X., Zhang, B., & Qiao, G. J. 2001, Astropart. Phys., 15, 101
Zane, S., Turolla, R., & Treves, A. 2000, ApJ, 537, 387